Charged Rod Aggregates and Neutral Coils of Polydiacetylene in Dilute Solution

Renliang Xu and Benjamin Chu*

Department of Chemistry, State University of New York at Stony Brook, Stony Brook, New York 11794-3400. *Received January 5, 1989*

ABSTRACT: Time dependence of the transition of coils to rod aggregates of P4BCMU in solvent mixtures of chloroform/toluene was investigated by means of laser light scattering and transient electric birefringence. The results show that the aggregates were formed in a short time (<1 h), but it took a much longer time (a few days) for the entire solution to reach an equilibrium. On the basis of the coexistence of neutral polymer coils and charged rodlike aggregates, novel electrophoretic separations of polydiacetylene (P4BCMU) in chloroform/toluene solvent mixtures were performed. The behavior of P4BCMU solutions in solvent mixtures with different solvent dielectric constants under an applied electric field was studied. The origin and the possible mechanisms for charge transfer of nonionic polymer molecules in nonaqueous dispersions were discussed by applying Coehn's empirical law.

I. Introduction

Polydiacetylenes ($(=CR—C\equiv C—CR=)_n$) are prototype conducting polymers whose applications in materials science have become significant because of their many interesting properties, such as the large quasi-one-dimensional structure of their single crystals, the high third-order optical susceptibility, the large optical nonlinearity, and the high photoconductivity. The color change of polydiacetylenes associated with either the solid-state polymerization by γ-radiation or the conformational change in solution can be used to monitor any one of the following ambient parameters: time–temperature exposure, humidity, pressure, radiation exposure, pH, and gas exposure.[1] Polydiacetylenes have been used as a film waveguide in interferometers.[2] The potential uses of polydiacetylenes as an optical memory and information processor, utilizing the photoinduced isomerization of the acetylenic and butatrienic forms and the optical nonlinearity, have also been explored.[3]

After the first soluble polydiacetylene was synthesized a decade ago,[4] there have been extensive studies on the conformational properties of soluble polydiacetylene derivatives. The unique property to which most attention has been paid is the peculiar color change and size variation of polydiacetylenes in solution at different temperatures or solvent conditions. For example, when P4BCMU (poly[5,7-dodecadiyne-1,12-bis[(4-butoxycarbonyl)-methylurethane]], or systematically named poly[1,2-bis-[4-[[[(2-butoxy-2-oxoethyl)amino]carbonyl]oxy]butyl]-1-buten-3-yne-1,4-diyl], with bulky, sufficiently flexible and polar substituent groups R = $(CH_2)_4OCONHCH_2CO-OC_4H_9$) is dissolved in chloroform, it forms a yellow solution with a blue shift in the optical absorption peak from $\lambda_{max} \approx 625$ nm of the original crystalline state to $\lambda_{max1} \approx$ 460–470 nm. Dramatic reversible color change—from yellow to red with an additional absorption peak at $\lambda_{max2} \approx$ 520–550 nm—occurs by adding a poor solvent, toluene, to P4BCMU/$CHCl_3$ solution. A similar phenomenon is observed when P4BCMU is dissolved in toluene. At high temperatures, the solution is yellow, and at lower temperatures, it becomes red. The additional long-wavelength absorption indicates that the local electron configuration of the P4BCMU molecules has changed to a longer π-conjugation; e.g., they are partially elongated. Figure 1a shows typical absorption spectra from a P4BCMU (M_w = 1.2×10^5 g/mol) sample (A) in chloroform/toluene solvent mixtures. Associated with the color change, it has been found in many experiments that the size of P4BCMU molecules depends on solution color. The conformations of soluble polydiacetylenes in good solvent and poor solvent have been found, respectively, to be neutral wormlike coils of small overall size (a few hundred angstroms [for sample A]) with a fairly broad size distribution and charged rigid rodlike aggregates with a narrow particle size distribution. In a toluene/$CHCl_3$ solvent mixture the transition occurred when the mole fraction of chloroform in the chloroform/toluene mixed solvent (X_c) <0.45. The size of the aggregate (up to a few thousand angstroms) depends on the solvent composition and the polymerization number of P4BCMU. In pure toluene solution the average aggregation number depends on the polymer molecular weight.[5,6]

In this article we shall present the results of the time dependence of the absorption spectrum and the structure in the coil-to-rod transition of P4BCMU in chloroform/toluene mixtures at room temperatures by employing three optical techniques, i.e., laser light scattering (LLS), transient electric birefringence (TEB), and optical absorption. The results showed that it took a short time period (<1 h) to form aggregates, while a much longer time was needed (~1 week) for the whole solution to reach equilibrium when $X_c = 0.37$. When the TEB experiment of P4BCMU was performed in dilute solution, it was found, as first noticed by Zacher,[7] that P4BCMU in chloroform/toluene mixed solvent was positively charged, which resulted in a net macroscopic motion of the charged aggregates toward the negative electrode. A novel electrophoretic separation of P4BCMU in the solvent mixture was used to separate the charged rod aggregates from the neutral coils by application of an external electric field. Then, the red solid on the electrode and the leftover yellow solution could be characterized independently by means of LLS. The possible mechanism and the origin for the abnormal charge transfer are discussed in terms of the dielectric constant difference between the solvent and the polymer molecules.

II. Experimental Aspects

The P4BCMU samples (A and B) were synthesized using a synthetic route similar to the one reported by Patel et al.[8] and obtained courtesy of Drs. R. R. Chance and D. G. Peiffer at Exxon Research and Engineering Co. Molecular parameters of samples A and B in terms of the weight-average molecular weight (M_w), the radius of gyration (R_g), and the hydrodynamic radius (R_h) are listed in Table I under the column denoted by solution I. These parameters were obtained from dilute solutions of P4BCMU in chloroform by static and dynamic LLS. Both samples were found to be polydisperse ($M_w/M_n \approx 2.2$) with broad molecular weight distributions (MWD) when dissolved in pure chloroform. However, the MWD (or size distribution) became surprisingly narrow

* Author to whom all correspondence should be addressed.

0024-9297/89/2222-4523$01.50/0

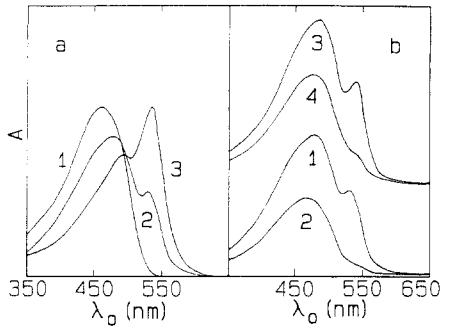

Figure 1. Absorption spectra for P4BCMU solutions after equilibration. Absorbance A (in arbitrary units) denotes the ordinate. In Figure 1a: 1, sample A in chloroform; 2, sample A in a chloroform/toluene mixture with $X_c = 0.41$; 3, sample A in toluene. It should be noted that the absolute scales of A for the three spectra (1–3) are different. In Figure 1b: 1, sample A before applying the electric field; 2, sample A after applying the electric field; 3, sample B before applying the electric field; 4, sample B after applying the electric field. Curves 1–4 have the same solvent composition of $X_c = 0.41$ and the same ordinate scale. Sample A has $M_w = 1.2 \times 10^5$ g/mol. Sample B has $M_w = 2.5 \times 10^6$ g/mol. The molecular properties of both samples in chloroform are listed in Table I.

Table I
Molecular Properties of P4BCMU in Chloroform

		solution[a]		
		I	II	IV
sample A	R_h, cm	1.7×10^{-6}	1.5×10^{-6}	2.0×10^{-6}
	R_g, cm	2.4×10^{-6}	2.1×10^{-6}	3.0×10^{-6}
	M_w, g/mol	1.2×10^5	1.0×10^5	1.7×10^5
sample B	R_h, cm	8.0×10^{-6}	4.2×10^{-6}	$(2.9 \times 10^{-6})^b$
	R_g, cm	1.1×10^{-5}	6.4×10^{-6}	$(3.7 \times 10^{-6})^b$
	M_w, g/mol	2.5×10^6	6.4×10^5	$(3.3 \times 10^5)^b$

[a] I, original samples; II, redissolution of the materials deposited on the electrode; IV, redissolution of the leftover materials in solution after the electrophoretic separation. [b] Polymer molecules may possibly have broken during the dry-out process. Uncertainties of measurements are $M_w \sim 5\%$, $R_g \sim 10\%$, and $R_h \sim$ a few percent.

once the solution started to change from yellow to red. Rodlike aggregates were formed in chloroform/toluene mixtures when $X_c < 0.5$.[5] Table II lists the characteristic absorptions and their relative magnitudes for samples A and B in solutions of three typical solvent compositions at room temperatures after the solutions have been equilibrated for a few days.

A specially designed, fully automated prism-cell LLS apparatus with a 50-mW He–Ne laser operated at $\lambda_0 = 632.8$ nm as the light source and with five detectors was employed to perform static and dynamic LLS, as well as to monitor the refractive index of the solution, simultaneously.[9] At $\lambda_0 = 632.8$ nm the solution absorption was negligible. A photomultiplier tube (PMT1) was located at a large scattering angle ($\theta = 87°$) while another photomultiplier tube (PMT2) was located at a small scattering angle ($\theta = 4.4°$); a photodiode array detector, from which the time-average scattered intensity was measured, was centered at $\theta = 24.6°$ and covered an angular range from ~20° to ~48°; a lateral position detector (D1) was used to monitor the laser intensity and the incident beam direction fluctuations; and a second lateral position detector (D2) was used to monitor the refractive index of the solution by measuring the direction of the transmitted beam, which was refracted by the prism–solution and prism–air interfaces.

The normalized intensity–intensity correlation function from the self-beating dynamic LLS is[10]

$$(G^{(2)}(\tau)/A - 1) \approx \beta\left[\left(\frac{I - I_0}{I}\right)|g^{(1)}(\tau)|\right]^2 = \beta\left[\left(\frac{I - I_0}{I}\right)\int_{\Gamma_{min}}^{\Gamma_{max}} G(\Gamma)\exp(-\Gamma\tau)\,d\Gamma\right]^2 \quad (1)$$

Table II
Characteristics of Absorption Spectra of P4BCMU in Chloroform/Toluene Solvent Mixtures

			before[c]	after[c]	
sample A	X_c	1.0	0.41	0.41	0.0
	λ_{max1},[a] nm	460	475	465	490
	λ_{max2},[a] nm		530	530[b]	535
	$A_{\lambda_2}/A_{\lambda_1}$	0	0.61	0.13	1.4
sample B	X_c	1.0	0.41	0.41	0.0
	λ_{max1},[a] nm	468	485	475	495
	λ_{max2},[a] nm		540	540[b]	542
	$A_{\lambda_2}/A_{\lambda_1}$	0	0.61	0.21	1.6

[a] Absorption maximum measured to ~±1 nm. [b] Only a shoulder in the absorption spectrum was observed, as shown in Figure 1b (curves 2 and 4). [c] Before and after denote the same solution before and after electrophoretic separation of charged rodlike particles from neutral coils.

with $g^{(1)}(\tau)$, I_0, I, τ, A, Γ, $G(\Gamma)$, and β being the normalized electric field correlation function, the solvent scattered intensity, the solution scattered intensity, the delay time, the base line, the characteristic line width, the normalized characteristic line width distribution function, and an instrument beating efficiency coefficient, respectively. The correlation data were fitted by the cumulants method.[11] In the small scattering angle limit, Γ is related to the translational diffusion coefficient D_T ($=\Gamma/K^2$, $\mathbf{K}$ is the scattering vector related to the scattering angle θ, the wavelength of light in vacuo λ_0, and the refractive index of the solution n by $K = 4\pi n \sin(\theta/2)/\lambda_0$).

The scattered intensity data recorded from static LLS at small scattering angles obey the relation

$$\frac{I_0}{I - I_0} \approx (H'(\partial n/\partial C)_{T,P}^2 C M_w)^{-1}\left[1 + \frac{1}{3}K^2\langle R_g^2\rangle_z\right] + \frac{2A_2}{H} \quad (2)$$

with C, M_w, A_2, $\langle R_g^2\rangle_z$ ($\equiv R_g^2$ hereafter for simplicity), H', and $(\partial n/\partial C)_{T,P}$ ($\equiv \partial n/\partial C$ hereafter for clarity) being the solution concentration, the weight-average molecular weight, the second virial coefficient, the mean-square z-average radius of gyration, an optical constant, and the refractive index increment; $H = H'(\partial n/\partial C)^2$. In a dilute solution with the mass concentration on the order of 10^{-5} g/mL, the last term in eq 2 is expected to be much smaller than the first term and can be omitted without introducing a large error. As the contribution to the total scattered light intensity from single coils is much less than rodlike aggregates, the effective concentration C, $\partial n/\partial C$, and M_w are possible variables for a solution undergoing the transition. Thus, a plot of $(I(\theta,t)/I_0(\theta) - 1)^{-1}|_{\theta\to 0}$ versus time tells us what has happened to the term $(\partial n/\partial C)^2 C M_w$ as a whole. If $\partial n/\partial C$ under a constant chemical potential was known from a plot of $(I(\theta,t)/I_0(\theta) - 1)^{-1}$ versus K^2, R_g and M_w can be obtained from the slope and the intercept after corrections for concentration effect and for molecular anisotropy.[12] M_w becomes the molar mass for aggregates.

TEB measurements were performed by our automated TEB apparatus with a 15-mW He–Ne laser operating at $\lambda_0 = 632.8$ nm as the light source.[13] As P4BCMU could be plated out at the negative electrode under certain solvent conditions, all TEB data were recorded by applying the electric field only once in order to avoid concentration change due to deposit of the polymer at the negative electrode, i.e., without scan averaging. The recorded time-dependent transmitted intensity $I_{tr}(t)$ from TEB measurements are converted to time-dependent optical retardation $\delta(t)$ ($\equiv 2\pi l\Delta n(t)/\lambda_0$, with l and $\Delta n(t)$ being, respectively, the effective electrode length and the solution birefringence) according to

$$I_{tr}(t) = JI_p \sin^2(\alpha + \delta(t)/2) + I_s \quad (3)$$

where I_p, I_s, J, and α are the incident light intensity polarized at 45° with respect to the horizon, the intensity of stray light including dark counts from the PMT, an intensity loss factor resulting from absorption, reflection, and scattering, and a deviation angle from the cross position of the last polarizer, respectively. The amplitude of optical retardation δ and the relaxation rate τ^{-1} ($=6D_R$ with D_R being the rotational diffusion

Table III
Approximate Time Needed To Reach Color Equilibration of P4BCMU in Chloroform/Toluene Solvent Mixtures

				Sample A					
X_c	1.0	0.63	0.43	0.40	0.36	0.30	0.21	0.024	0.0[b]
time,[a] h	0	2	2	34	74	34	34	2.4	1
				Sample B					
X_c	1.0	0.39	0.37	0.35	0[b]				
time,[a] h	0	220	140	120	2				

[a] Equilibration time was established when A_{540} remained constant to ±0.5% of its final value. Initial time delay uncertainty was about ≲10 min. For long equilibration time, the time was rounded to the hour unit. [b] Dissolution of the polymer was at ~70 °C.

coefficient) of the field-free decay in TEB measurements are related

$$\delta(t) = \delta_0 \exp(-t/\tau) = (4\pi^2\phi_2\Delta g\Phi l/\lambda_0 n) \exp(-t/\tau) \quad (4)$$

with δ_0, ϕ_2, Φ, and Δg being, respectively, the amplitude of δ at the time the electric field is switched off (t = 0), the volume fraction of the anisotropic solute, an orientation function whose value approaches 1 in high fields, and the optical anisotropy factor of the solute.

Optical absorption was recorded by using a GCA/McPherson 700 Series double-beam UV–visible spectrophotometer. Chloroform was used as the reference, and the spectra were scanned from 350 to 650 nm.

III. Time Dependence

The color, as well as the scattered intensity and the solution birefringence of various P4BCMU solutions in chloroform/toluene with different X_c values, would change continuously for days. By tracing the absorption maximum at $\lambda_0 \approx 540$ nm as a function of time, we found the slowest change when chloroform and toluene were competitive in a region of $X_c \sim 0.35$–0.40, as shown in Table III.

The solvent composition chosen in the present time-dependence measurements was $X_c = 0.368$ with polymer sample B mass concentration $C = 1.3 \times 10^{-5}$ g/mL. The polymer was first dissolved in chloroform. Toluene was then subsequently added to the chloroform solution in order to reach the desired solvent composition and polymer concentration. The time for dissolution was discounted. Thus, the starting time (t = 0) was precise to about a few minutes. All measurements were performed at 24 °C. The solution was introduced into the prism cell by a circulation system[9] through a 0.5-μm pore diameter Millipore filter. At $X_c = 0.368$, the absorption peak at $\lambda_{max1} = 483$ nm was being shifted continuously to $\lambda_{max1} = 495$ nm and the amplitude was being reduced with increasing time, while the second peak position ($\lambda_{max2} = 540$ nm) remained unchanged but the amplitude (A_{540}) was almost tripled during the 5-day measurement time period. The growth of A_{540} indicates an increasing amount of the longer conjugation as a function of time; i.e., some molecules have been partially stretched, and parts of these molecules now have longer π-conjugation. All extensive parameters, such as the scattered light intensity, the amplitude of birefringence, and the amplitude of the absorbance A_{540} (see, for example, A_{540}/C as denoted by hollow inversed triangles in Figure 2), followed, after an initial period of ~1 h, an empirical equation $Y(t) - Y(\infty) = A \exp(-t/\tau)$ where $Y(t)$ was an extensive parameter at time t, A was an amplitude constant, and $\tau \sim 43$ h. The results were reproducible in the dilute solution region. If the absorbance of the solution at $\lambda_0 = 540$ nm was used to scale the extensive values, time-independent relations could be obtained for the scattered light intensities from both small and large scattering angles and for the solution birefringence as displayed typically by the hollow diamonds in Figure 2. The aggregation changes the particle weight, the anisotropy factor Δg, and possibly the refractive index increment

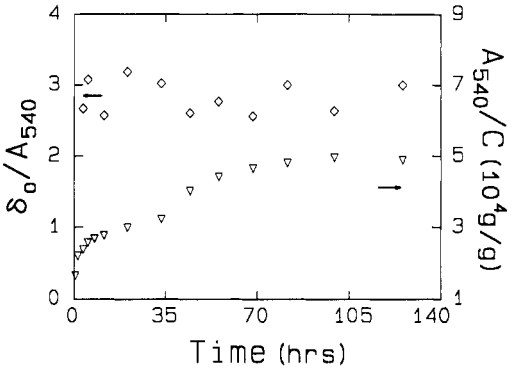

Figure 2. Concentration-scaled absorbance, A_{540}/C (inverted triangles), and absorbance-scaled birefringence amplitude, δ_0/A_{540} (diamonds), as a function of time for sample B at $X_c = 0.368$ and $C = 1.3 \times 10^{-5}$ g/mL.

$\partial n/\partial C$. These changes produce an increase in both the scattered intensity and the depolarized transmitted intensity. Two simplified routes for the growth process can be proposed. The aggregates could grow continuously while more aggregates were being formed or only a certain size range of aggregates were permissible, but more aggregates of the same size were being formed with increasing time. To distinguish the two possible paths, intensive parameters, such as the diffusion coefficients, were examined.

The intensive parameters, such as translational and rotational diffusion coefficients and the radius of gyration, were essentially time independent after an initial time period of ~0.5 h. The constant intensive properties during the whole measurement period of tens (or hundreds) of hours imply that the route of continuing size growth of aggregates, as mentioned above, could be ruled out. The size of the aggregates could be estimated as follows. If we took the aggregates to be rods or prolate ellipsoids (pe) and used the average R_g and D_T values, we got lengths (L) and diameters (d) as follows: $\langle L\rangle_{rod} = 7.2 \times 10^{-5}$ cm, $\langle L\rangle_{pe} = 9.2 \times 10^{-5}$ cm, $\langle d\rangle_{rod} = 6.6 \times 10^{-6}$ cm, and $\langle d\rangle_{pe} = 9.0 \times 10^{-6}$ cm, with both R_g and D_T as functions of the long-axis dimension and the ratio of the long axis to the short axis, respectively.[14,15] A systematic investigation of the size variation of P4BCMU in toluene/chloroform dilute solutions at various solvent compositions have been carried out.[5]

Single P4BCMU molecules, when in the coil state, are small in size with R_g equal to approximately a few hundred angstroms.[5] Thus, they are weak scatterers and do not have any appreciable birefringence. Under a poor solvent condition the polymer molecules tend to become flat or locally stretched, i.e., have a longer π-conjugation. The change not only causes a solvatochromic change in the absorption spectra but also results in an aggregation of the stretched-out polymer molecules. The aggregation occurs over a relatively short time scale (<1 h). On the other hand, the overall coil-to-rod transition reaches an equilibrium state very slowly. The number concentration of

aggregates thus increases with time, and the concentration increase is responsible for the increase in all the extensive parameters; but the average size of the aggregates does not change, as shown by the values of the intensive parameters. Muller et al.[16] found that the $\partial n/\partial C$ value for P4BCMU in toluene when extrapolating to the dilute solution region was less than twice that in chloroform at $\lambda_0 = 633$ nm. By tracing the refractive index change using the prism-cell light-scattering apparatus, we did find a drift of the refractive index of the solution. In the first approximation, the light spot position change on the D2 detector is proportional to the solution refractive index change. In our dilute solution case $\Delta n \approx (\partial n/\partial C)C$ where C is the weight concentration of aggregates. If the excess scattered intensity is scaled by the D2 position change, we have

$$\{(I/I_0 - 1)/(P_{D2} - P_{D2}(t = 0))\}_{K\to 0} \approx \{H'(\partial n/\partial C)^2 C M_w\}/\{(\partial n/\partial C)C\} = H'(\partial n/\partial C)M_w \quad (5)$$

Such a plot showed that $(\partial n/\partial C)M_w$ was a constant, at least in the first approximation. Thus, after an initial period, the scattered intensity change was mainly due to the concentration change of the aggregates not due to either the refractive index change of the polymer molecules or the growth in the aggregate size.

IV. Electrophoretic Separation and Charge Transfer

Three typical solvent compositions were chosen in the electrophoretic separation experiments; i.e., $X_c = 0$, 0.41, and 1 (the symbol 1 denotes solution I in Table I). When the P4 BCMU polymer was dissolved in chloroform, there were neither substances deposited on either of the two electrodes nor an appreciable birefringence signal in the presence of an applied electric field with field strength up to 6 kV/cm. On the other hand, macroscopic electrophoretic motion and substantial deposit of a red substance to the negative electrode occurred when the electric field was applied to solutions with solvent mixture compositions of $X_c \lesssim 0.41$. When the P4BCMU polymer was dissolved in toluene ($X_c = 0$), the red solution could be made into a colorless liquid by continuous application of an external electric field and all the P4BCMU polymer was deposited at the negative electrode, which turned reddish. Thus, the red color was due to the positively charged P4BCMU, which formed rodlike aggregates as evidenced by the much higher R_h and R_g values for P4BCMU in toluene.[5] It was obvious from Table II that, even when all polymers had formed rodlike aggregates, there remained an absorption at $\lambda_{max} = 490$ nm, which was similar to the one that appeared in solutions of P4BCMU in chloroform ($\lambda_{max} = 460$ nm). One might assume that there was still some local characteristic "yellow" π-conjugation in the polymer chain, but the local rigidity change caused the red absorption to be shifted by ~25–30 nm. However, Chance showed that this absorption had the same origin as $\lambda_{max} = 542$ nm when comparing the absorption spectra of polydiacetylene in poor solvent with that of its crystal form.[17]

In solutions at $X_c = 0.41$, the electric field strength required was much higher than that in pure toluene. We used $E = 3$ kV/cm for sample A and $E = 6.5$ kV/cm for sample B instead of $E = 0.6$ kV/cm for both samples in pure toluene. After electrophoretic separation, the solution turned yellow and had some residues of aggregates, as shown in Figure 1b and listed in the column denoted by "after" in Table II. However, the sample A solution was "clearer" than the sample B solution regarding the reddish tint in the yellow solution. In a comparison of the curve 2 in Figure 1b with the curve 1 in Figure 1a, we found that the remaining yellow solution had an absorption maximum red-shifted by ~5 nm. This could be due to the rigidity change of polymer molecules under different solvent conditions.[18] Thus, the experiments have demonstrated that neutral coils and charged rods coexist at $X_c = 0.41$ and that charged rods can be separated from the neutral coils by applying an external electric field. The oxidation of polymer molecules was negligible since the red materials that were deposited on the electrode could be redissolved in chloroform to form a yellow solution and the solution was neutral again.

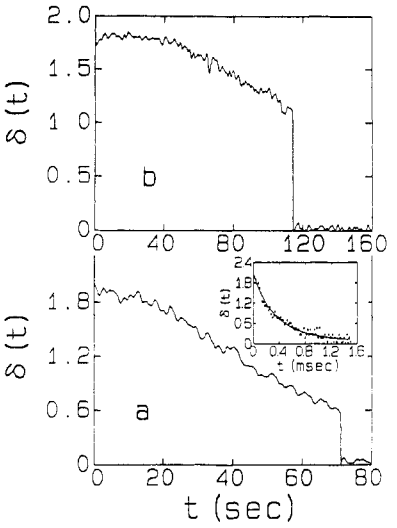

Figure 3. Optical anisotropy $\delta(t)$ versus time for sample A (a) and sample B (b) at $X_c = 0.41$ using square pulses of pulse widths 71 and 114 s, respectively. A software low-frequency-pass filter has been used to smooth the data. The slopes of the curves (a) and (b) are 2.4×10^{-2} and 9.2×10^{-3} deg/s, respectively. The inset in (a) is a free decay after switching off the electric field from a transient electric birefringence measurement (an enlargement of the sharp drop in (a)); the average rotational diffusion coefficient of the rodlike particles D_R (=462/s) can be computed from the field-free decay using a cumulants fitting procedure.

For the same material in high fields where particles are fully oriented, the measured optical anisotropy δ is proportional to the volume fraction of the anisotropic solute (eq 4 with $\Phi \approx 1$ and Δg being a constant for the same material). From measurements of the amplitude of the solution birefringence the reduction of the red aggregates in solution as a function of the field-on time could be monitored. Figure 3 shows two typical curves of the solution anisotropy $\delta(t)$ as a function of time. The red P4BCMU polymer could be removed from the solution at different rates even in the above-mentioned (different) field strengths. Sample A had a δ reduction rate of 2.4×10^{-2} deg/s at $E = 3$ kV/cm after a short flat region; while sample B had a rate of 9.2×10^{-3} deg/s at $E = 6.5$ kV/cm after the flat region. The reduction rate depends on solvent composition (and possibly on electric field strength). The red substance deposited on the negative electrode could easily be redissolved in chloroform to form a yellow solution (solution II in Table I). Solution II did not show any particle electrophoretic motion that ruled out the possibility of polymer oxidation in the electrodes when they were deposited from solution I. The polymer in the leftover yellow solution (solution III) was dried out from the solvent and redissolved in chloroform (solution IV in Table I). Solutions I ($X_c = 1$), II, and IV were then characterized by means of LLS. The results are listed in Table I.

The original γ-radiation synthesized polymers have broad molecular weight distributions (MWD). The observation that no further color change in solution III was

observed in a time period of weeks and that solution III could become red again only by adding more toluene demonstrated that only polymers of certain sizes could be straightened out to have a large π-conjugation in a given solvent quality. Furthermore, smaller molecules were being straightened first as the solvent condition became poorer, as shown by the results listed in Table I.

It should be noted that this finding differs with the observation involving a decrease in the color transition temperature in pure toluene with decreasing molecular weight.[6] The discrepancy could be due to the difference in solvent quality between pure toluene and the mixed solvent or due to the differences in electrophoretic mobility of the aggregates. We could, however, rule out the second possibility because we did separate all the charged rods from the neutral coils at a certain solvent quality.

It has been found that liquid hydrocarbons or particles dispersed in nonaqueous liquids can have stable excess electronic charge carriers formed by impurities or any kind of radiation, such as γ-rays.[19,20] The generally accepted possible origins of the surface charge in nonaqueous dispersions are preferential adsorption of dissociated cations or anions and the dissociation of any dissociative group on the surface. However, experimental evidences for charge transfer from the above origin are rare. To our knowledge, it has not been reported for nonionic polymers, other than polydiacetylene, dissolved in an organic solvent to be a charge carrier. According to Coehn's empirical law, substances of higher dielectric constant (ϵ) will take a positive charge when brought into contact with substances having a lower dielectric constant.[21] In comparing the dielectric constant (ϵ) of different solvents used in the P4BCMU study, we have found that the dielectric constants of both toluene (ϵ = 2.4) and *n*-hexane (ϵ = 1.9) are relatively small while chloroform has a dielectric constant ϵ of 4.8. If Coehn's law is valid, then the charge status of P4BCMU in a solvent mixture must be related to the dielectric constant of the solvent. Several poor solvents of P4BCMU at room temperatures were mixed with chloroform to form P4BCMU dilute solutions. The solvent composition was adjusted such that all solutions were visually orange, implying the coexistence of unstretched and partially stretched P4BCMU molecules in the solvent mixtures. When the poor solvent had a ϵ value of <2.5, the P4BCMU solute behaved similarly; i.e., they had electrophoretic motion toward the negative electrode and showed strong scattered intensity and strong birefringence. In a chloroform/ethyl acetate solution there was neither electrophoretic motion nor any birefringence signal even though the solution had a very strong absorption at λ_0 = 530 nm with $A_{530}/A_{485} \sim 1$. In a chloroform/nitromethane solution ($\epsilon_{\text{nitromethane}} \approx 36$), on the contrary, the polymer became *negatively* charged. The red substance at the *positive* electrode from the solution using chloroform/nitromethane as the mixed solvent was very difficult to be redissolved in chloroform, and we could not yet find a good explanation for this behavior. Nevertheless, the dielectric constant of the solvent appeared to play an important role in the charger-transfer process. Table IV lists the results of the field-on test for various solvent mixtures having different values of the dielectric constant.

It can be suggested that P4BCMU polymers are potentially charge carriers possibly due to the history of γ-radiation and the long π-conjugation. When contacting with solvent molecules of different dielectric constants, the residue ions or impurities will induce charge transfer, which obeys Coehn's law. The phenomenon could also be qualitatively explained by a simple model based on the partition coefficient.[22] The longer π-conjugation reduces the electron energy level and makes it easier for charge transfer to take place when compared with the shorter π-conjugation. Thus, the straightening out of molecules from yellow neutral coils to red charged rods promotes the aggregation of rodlike molecules. On the other hand, the aggregation could further reduce the electron energy level and make the charge transfer easier. Otherwise, even if the polymer molecule is straightened out, the molecules cannot form rodlike aggregates without the charge carriers. In the solvent conditions of our experiments the coils are neutral. If the charges are located at the ends of polymer chains, as suggested by Zacher[23] and smaller polymers have more ends than larger ones, then the aggregates formed by sample A have a higher charge density than those of the aggregates formed by sample B. This can explain the different reduction rates for the two samples as shown in Figure 3.

Table IV
Charge Status of P4BCMU in Solvents of Different Dielectric Constant

solvent	X_c[a]	ϵ	μ	charge sign[b]	sign of δ
n-hexane	0.5	1.9	0.09	+	+
carbon tetrachloride	0.23	2.2	0.00	+	+
toluene	<0.4	2.4	0.31	+	+
chloroform	1.0	4.8	1.2	0	0
ethyl acetate	<0.09	6.0	1.8	0	0
nitromethane	0.19	36	3.6	−	+

[a] Tests were performed to both samples A and B. X_c values listed are for sample A. [b] Charge sign is defined such that when the red substance is deposited at the negative electrode, the charge sign is positive: ϵ, dielectric constant; μ, dipole moment in debye; δ, optical anisotropy.

V. Conclusion

By employing the prism-cell LLS spectrometer with five detectors and the TEB apparatus, we have obtained a general view of the conformational transformation of P4BCMU polymer molecules in chloroform/toluene solutions. In contrast to earlier findings[24-26] using the same TEB approach, our use of mixed solvent from pure chloroform to pure toluene could reveal how neutral coils changed to rod aggregates by a more delicate variation of the solvent quality. The polymer molecules (e.g., sample A) in chloroform have a broad size distribution and are single wormlike coils with a hydrodynamic radius (R_h) of a few hundred angstroms. By adding a poor solvent, toluene, to the solution, the local configuration of the molecule starts to change, a longer π-conjugation with an additional absorption peak located at $\lambda_{max2} \approx 540$ nm, and the polymer molecules tend to become stiffer or locally more stretched. Charge transfer can occur because of the dielectric constant difference between the solvent and the polymer. The stiffer charged polymer molecules then become aggregated, which are best described as rodlike aggregates with an almost-uniform size when $X_c < 0.43$. The aggregation occurs over a relatively short time scale (<1 h). However, the time period for the solution color change and the molecular shape conversion to be equilibrated depends on the solvent composition and can take from a few hours to a few hundred hours. In a certain solvent condition the neutral coils and the charged rods can coexist. This property can be utilized as a new approach for fractionation of such materials. The process may be fine-tuned by controlling the solvent quality.

Acknowledgment. We thank Drs. R. R. Chance and D. G. Peiffer for providing the P4BCMU samples, Dr. R. A. Zacher for sending us the preprints, and Prof. Z. Zhou for helpful discussions. B.C. wishes to acknowledge support of this work by the National Science Foundation Polymers Program (DMR8617820).

Registry No. P4BCMU (homopolymer), 68777-93-5; P4BCMU (SRU), 76135-61-0.

References and Notes

(1) Prusik, T.; Montesalvo, M.; Wallace, T. *Radiat. Phys. Chem.* **1988**, *31*, 441.
(2) Singh, B. P.; Prasad, P. N. *J. Opt. Soc. Am. B: Opt. Phys.* **1988**, *5*, 453.
(3) Hanamura, E.; Itsubo, A. *Proc. SPIE-Int. Soc. Opt. Eng.* **1988**, *824*, 66.
(4) Patel, G. N. *Polym. Prepr.* **1978**, *19*, 154.
(5) Chu, B.; Xu, R. *Macromolcules* **1989**, *22*, 3153.
(6) Rawiso, M.; Aime, J. P.; Fave, J. L.; Schott, M.; Muller, M. A.; Schmidt, M.; Baumgartl, B.; Wegner, G. *J. Phys. Fr.* **1988**, *49*, 861.
(7) Zacher, R. Ph.D. Thesis, University of California at Santa Barbara, 1987.
(8) Peiffer, D. G., private communication.
(9) Chu, B.; Xu, R.; Maeda, T.; Dhadwal, H. S. *Rev. Sci. Instrum.* **1988**, *59*, 716.
(10) Berne, B. J.; Pecora, R. *Dynamic Light Scattering*; Wiley: New York, 1976.
(11) Koppel, D. E. *J. Chem. Phys.* **1972**, *57*, 4814.
(12) Chu, B.; Xu, R.; DiNapoli, A. *J. Colloid Interface Sci.* **1987**, *116*, 182.
(13) Xu, R.; Ford, J.; Chu, B. In *Particle Size Distribution: Assessment and Characterization*; Provder, T., Ed.; ACS Symp. Series 332; American Chemical Society: Washington, DC, 1987; pp 115-132.
(14) Newman, J.; Swinney, H. L.; Day, L. A. *J. Mol. Biol.* **1977**, *116*, 593.
(15) Tanford, C. *Physical Chemistry of Macromolecules*, Wiley: New York, 1961.
(16) Muller, M.; Schmidt, M.; Wegner, G. *Makromol. Chem., Rapid. Commun.* **1984**, *5*, 83.
(17) Chance, R. R. *Macromolecules* **1980**, *13*, 396.
(18) Aime, J. P.; Rawiso, M.; Schott, M. *Springer Ser. Solid-State Sci.* **1987**, *76*, 58.
(19) Minday, R. M.; Schmidt, L. D.; Davis, H. T. *J. Chem. Phys.* **1971**, *54*, 3112.
(20) Kitahara, A., Watanabe, A., Eds. *Electrical Phenomena at Interfaces*; Marcel Dekker: New York, 1984; p 118.
(21) Coehn, A.; Raydt, V. *Ann. Phys. (Leipzig)* **1909**, *30*, 777.
(22) Zhou, Y.; Stell, G.; Friedman, H. L. *J. Chem. Phys.* **1988**, *89*, 3836.
(23) Zacher, R. A. *J. Chem. Phys.*, in press.
(24) Lim, K. C.; Kapitulnik, A.; Zacher, R.; Heeger, A. J. *J. Chem. Phys.* **1985**, *82*, 516.
(25) Schmidt, M.; Wegner, G. *J. Chem. Phys.* **1986**, *84*, 1057.
(26) Lim, K. C.; Kapitulnik, A.; Zacher, R.; Heeger, A. J. *J. Chem. Phys.* **1986**, *84*, 1058.

Intrinsic Dynamic Viscoelasticity of Polystyrene in Θ and Good Solvents

Dennis W. Hair and Eric J. Amis*

Department of Chemistry, University of Southern California, Los Angeles, California 90089-0482. *Received February 15, 1989; Revised Manuscript Received April 22, 1989*

ABSTRACT: Intrinsic dynamic storage and loss shear moduli have been measured for polystyrene in decalin (Θ solvent) and in toluene (good solvent) with a multiple-lumped resonator instrument. The Θ-solvent data can be fit with theory by assuming fully developed hydrodynamic interaction ($h^* = 0.25$) and Gaussian coils in the Rouse-Zimm bead-spring model. For the good solvent data two treatments are used to account for the influences of chain expansion. Fitting parameters are obtained from independent measurements of radius of gyration and intrinsic viscosity. Analyses are performed with (1) the Rouse-Zimm bead-spring model with Gaussian chain statistics and reduced hydrodynamic interaction ($h^* = 0.04$), (2) a modified Rouse-Zimm model, which includes statistics of expanded chains with an independent h^*, and (3) a scaling type approach, which incorporates chain expansion but does not explicitly modify a draining parameter. Although we cannot discriminate between the models, the influence of chain expansion on draining is demonstrated, as is the need to find a consistent treatment.

Introduction

Fujita has recently discussed[1] several examples of unsolved problems of polymer behavior in dilute solution. Areas of difficulty that he focused on are the magnitudes and molecular weight dependences of intrinsic viscosity, hydrodynamic factors, second virial coefficients, and the excluded-volume effect. His literature review pointed out the lack of adequate theoretical explanations, in terms of molecular parameters, for long-standing experimental results on intrinsic viscosity, radius of gyration, diffusion coefficient, sedimentation coefficient, second virial coefficient, and persistence length. For the special case of Θ conditions there is actually rather good predictive theory, but, as Fujita emphasizes, one fundamental problem that remains a key to understanding dilute solution behavior in general is the coupling between the diminution of intramolecular hydrodynamic interaction and the onset of polymer chain expansion as is precipitated by excluded-volume interactions. This coupling has previously been the subject of numerous experimental observations and theoretical treatments, particularly of intrinsic viscosity and hydrodynamic radius.[2-5]

This paper presents a new set of experimental results that illustrate this effect and require explanation. The studies are of intrinsic dynamic storage and loss shear moduli, $[G']_R$ and $[G'']_R$, of dilute flexible polymer solutions. The samples are well-characterized, nearly monodisperse, linear polystyrenes in both good solvent and Θ-solvent conditions. The data are compared to predictions from theoretical treatments that approach the problem from different sides of the hydrodynamic and excluded-volume influences.

It is well-known that the statistical radius of a polymer chain, for example, the radius of gyration, R_G, varies with molecular weight as $R_G \sim M^{\nu}$ where the excluded-volume

* Author to whom correspondence should be addressed.

0024-9297/89/2222-4528$01.50/0